DISCLAIMER

This document was prepared as an account of work sponsored by the United States Government. While this document is believed to contain correct information, neither the United States Government nor any agency thereof, nor the Regents of the University of California, nor any of their employees, makes any warranty, express or implied, or assumes any legal responsibility for the accuracy, completeness, or usefulness of any information, apparatus, product, or process disclosed, or represents that its use would not infringe privately owned rights. Reference herein to any specific commercial product, process, or service by its trade name, trademark, manufacturer, or otherwise, does not necessarily constitute or imply its endorsement, recommendation, or favoring by the United States Government or any agency thereof, or the Regents of the University of California. The views and opinions of authors expressed herein do not necessarily state or reflect those of the United States Government or any agency thereof or the Regents of the University of California.

Ice Formation in Gas-Diffusion Layers

Thomas Dursch,[a,b] C. J. Radke,[a,b] Adam Z. Weber[a]

[a]Lawrence Berkeley National Laboratory, 1 Cyclotron Rd, Berkeley, CA 94720

[b]Department of Chemical Engineering, University of California, Berkeley, CA 94720

Under sub-freezing conditions, ice forms in the gas-diffusion layer (GDL) of a proton exchange membrane fuel cell (PEMFC) drastically reducing cell performance. Although a number of strategies exist to prevent ice formation, there is little fundamental understanding of the mechanisms of freezing within PEMFC components. Differential scanning calorimetry (DSC) is used to elucidate the effects of hydrophobicity (Teflon® loading) and water saturation on the rate of ice formation within three commercial GDLs. We find that as the Teflon® loading increases, the crystallization temperature decreases due to a change in internal ice/substrate contact angle, as well as the attainable level of water saturation. Classical nucleation theory predicts the correct trend in freezing temperature with Teflon® loading.

Introduction

Proton-exchange membrane fuel cells (PEMFCs) in automotive applications must permit startup from sub-freezing temperatures, known as *cold-start*. Under sub-freezing conditions, water in the membrane electrode assembly (MEA) forms ice that drastically

reduces cell performance, and can shut down the cell by plugging the catalyst layer, thereby starving the electrochemical reaction of reactant gases (1). A number of strategies exist to prevent ice formation including using a heat source to keep the PEMFC above freezing and/or purging the MEA of water prior to startup (2,3). These strategies are not ideal, however, because an external heating source is costly and the PEM needs to be rehydrated upon startup.

In recent years, much research has focused on developing a stack-level model of cold-start with the goal of better understanding the effect of material properties and warming strategies on startup, as well as water movement and redistribution. Balliet and Newman (4), He and Mench (5), and Meng (6), provide one-dimensional and multi-dimensional models for water movement, frost heave, and cold-start. However, current fuel cell literature uses an expression for the rate of ice formation derived from soil literature, since at this time an expression for hydrophobic porous media does not exist. Once the fundamentals of ice formation within fuel-cell media are better understood and an appropriate rate equation is developed, the precision of current cold-start models will be increased.

The goals of this paper are to elucidate the effect of varying hydrophobicity and water saturation on the rate of ice formation in a gas-diffusion layer (GDL) and to develop a rate equation from theory that can be used to predict these effects. The rate of ice formation is experimentally investigated through differential scanning calorimetry (DSC) for a variety of commercial GDLs with varying amounts of Teflon[®] (PTFE) and levels of water saturation. Classical nucleation theory is used to model the phase transformation of water to ice within the GDL, which can then be validated by the experimental DSC data.

Experimental

Differential scanning calorimetry was used to assess the change in the rate of ice formation for GDLs with varying PTFE content and level of saturation. Three different commercial GDLs were investigated, each with varying PTFE loadings, as shown in Table I.

TABLE I. PTFE contents for each of the commercial GDLs used in the procedure.

Manufacturer	PTFE Content (wt%)
SGL 24 Series	0, 5, 10, 20, 30
Toray (SGL PTFE Deposition)	5, 20
Toray (FCE PTFE Deposition)	0, 10, 20, 30, 40, 50, 60

Evacuation

To improve the reproducibility of the experiments, each GDL was punched into a 5-mm diameter circle. The samples were saturated with Ultrapure Milli-Q® water in a vacuum chamber for 40 minutes at 35 torr. After evacuation, excess water was blotted from the surface of the GDL with Fisherbrand® weighing paper. Water content was determined from the difference between the sample weight before and after the evacuation procedure. For a porosity of 80% and a thickness of 190 μm, GDLs

containing less than 40 wt% PTFE were calculated to be between 60 and 80% saturated (consistent with measured capillary pressure-saturation data)(7). After evacuation, water loss from the sample is minimal. Water loss by evaporation is also negligible due to small sample surface area, and water does not spontaneously drain from the GDL, as supported by capillary pressure-saturation data. To determine the effect of varying PTFE content, the samples were evacuated at a constant pressure and then placed directly into the DSC. For samples with a fixed PTFE content, water saturation was varied as described in the next section.

Controlling Saturation

Water content within the GDL was varied following Gostick *et al.* (7). After evacuation, samples were placed directly on a hydrophilic membrane (Millipore, 0.22 μm PVDF #GVWP04700) positioned between two plastic disks. A 3.175 mm diameter plastic tube was used to connect to a 50 mL syringe to the base of the bottom disk. The stand was flooded with water to remove any air from within the system. To control the water content in the GDL, syringe height was raised and lowered to vary the hydrostatic pressure, which changes the amount of water withdrawn from the GDL. Water content was determined by comparing the weight of the sample prior to evacuation to the weight of the sample after water removal. Water content is converted to saturation by

$$S = \frac{V_{water}}{V_{dry}} = \frac{m_{water}}{m_{dry}} \frac{\rho_{dry}}{\varepsilon \rho_{water}} \qquad [1]$$

where S is the saturation, ε is the porosity, V is the volume, m is the mass, and ρ is the density, of the water and dry GDL. Porosity and sample density are calculated as a function of the PTFE fraction according to Lim and Wang (8).

Differential Scanning Calorimetry

After evacuation or water removal, water saturated GDL samples were placed immediately in TA Instruments Q20 Differential Scanning Calorimeter[®]. Samples were cooled and heated in one cycle of 10 °C/min, followed by four cycles of 2.5 ° C/min. The 10 °C/min cycle was used to standardize thermal history and was not included in the data analysis. Figure 1 shows a typical DSC curve for a 20 wt % PTFE Toray (SGL) GDL. Heat flow versus temperature curves were analyzed using *TA Universal Analysis* to find the freezing point, as well as the total amount of water frozen. The crystallization temperature is defined as the temperature at the onset of freezing, or the temperature at which the heat flow first begins to rise to a maximum. Due to the random nature of the pore network and PTFE loading, each GDL sample was run a minimum of two times.
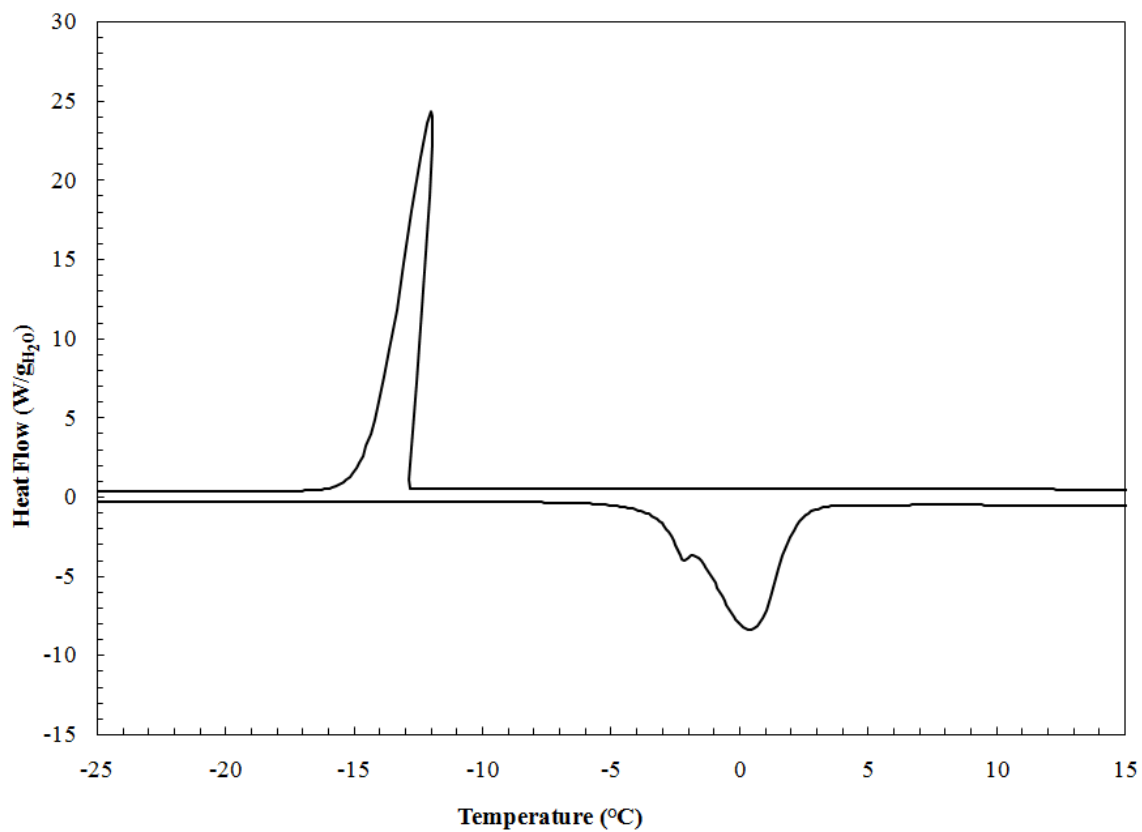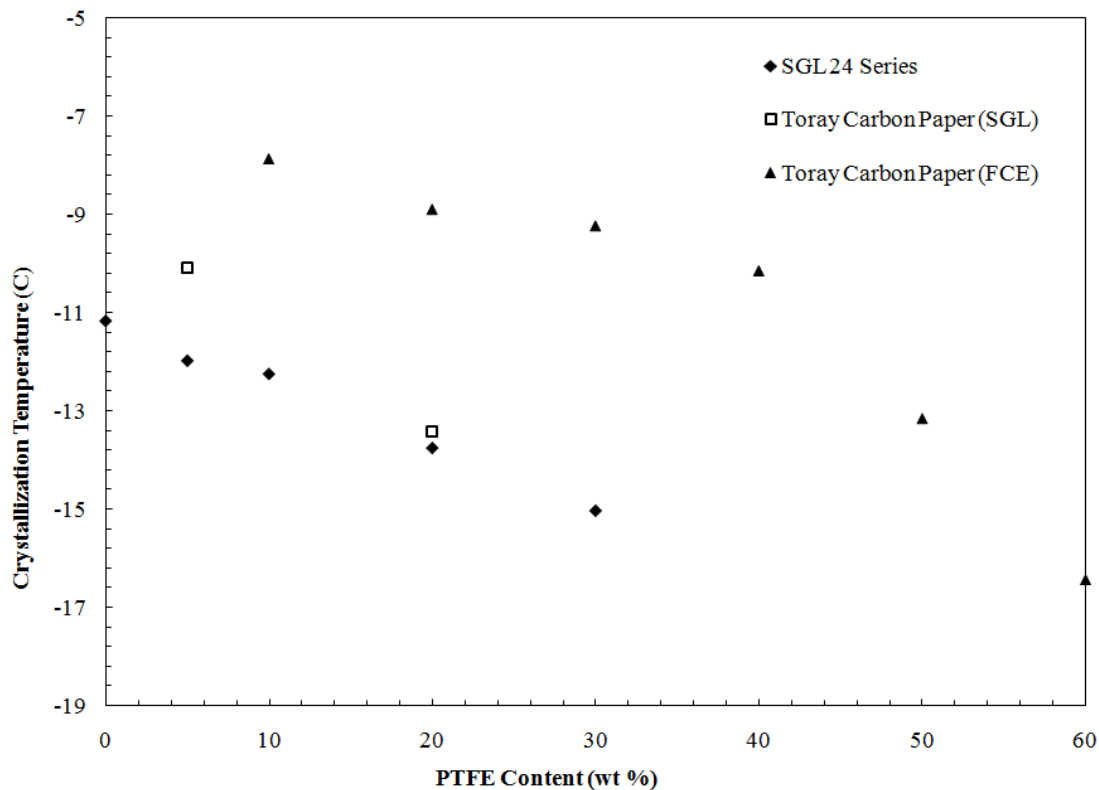
Figure 1. Crystallization temperature versus PTFE content for four commercial GDLs as measured by differential scanning calorimetry.

Results and Discussion

Figure 2 shows crystallization temperature versus PTFE content for the GDLs listed in Table I. For all GDLs, the crystallization temperature decreases as the PTFE content increases. Note that the SGL 24 and Toray (SGL) series GDLs follow a similar line, whereas water in the Toray (FCE) GDL freezes at a higher temperature. One possible

explanation is that the SGL 24 and Toray (SGL deposition) series GDLs have the same method of PTFE deposition, whereas the Toray (FCE) has a proprietary method of PTFE deposition. This observation suggests that the method of PTFE deposition influences the crystallization temperature. However, the overlying decrease in freezing temperature with higher PTFE contents remains the same.

Figure 2. Crystallization temperature versus PTFE content for four commercial GDLs as measured by differential scanning calorimetry.

We hypothesize that addition of PTFE to the porous network changes the average internal ice/substrate wettability (i.e., contact angle), as well as the attainable level of water saturation, causing the decrease in crystallization temperature. Although the PTFE takes up a finite volume in the porous network, mercury porosimetry results suggest that the addition of PTFE does not significantly change the pore-size distribution. Therefore, it is assumed that the pore-size distribution for all of the GDLs is relatively constant.

A plot of crystallization temperature and saturation versus PTFE content is shown for the Toray (FCE) series in Figure 3. For PTFE contents between 0 and 40 wt %, crystallization temperature decreases slightly with the addition of PTFE. Above 40 wt % PTFE, the crystallization temperature decreases more steeply. Between 0 and 40 wt % PTFE, water saturation remains relatively constant (within experimental error). However, those GDLs containing 50 and 60 wt% PTFE become increasingly difficult to saturate with water due to an increased capillary pressure. Consequently, saturation decreases abruptly. This suggests that at low enough fractions of PTFE, the saturation is constant and the average internal ice/substrate contact angle changes, while at larger fractions of PTFE, the attainable level of saturation also contributes to the decrease in crystallization temperature.
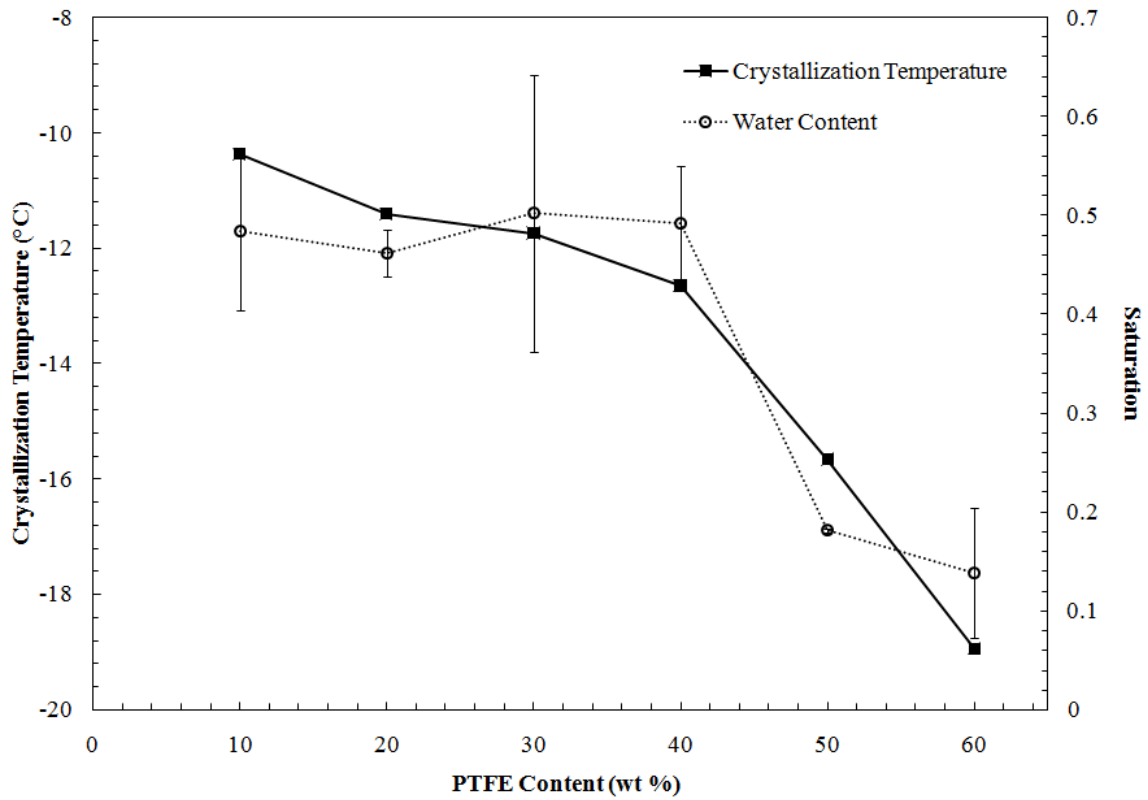
Figure 3. Crystallization temperature and saturation versus PTFE content for the Toray (FCE deposition) series from differential scanning calorimetry.

Figure 4 shows crystallization temperature versus saturation for an untreated (0 wt % PTFE) Toray GDL. As water saturation increases, the crystallization temperature also increases. One explanation is that at higher saturations, the transport resistance to crystal growth is reduced.
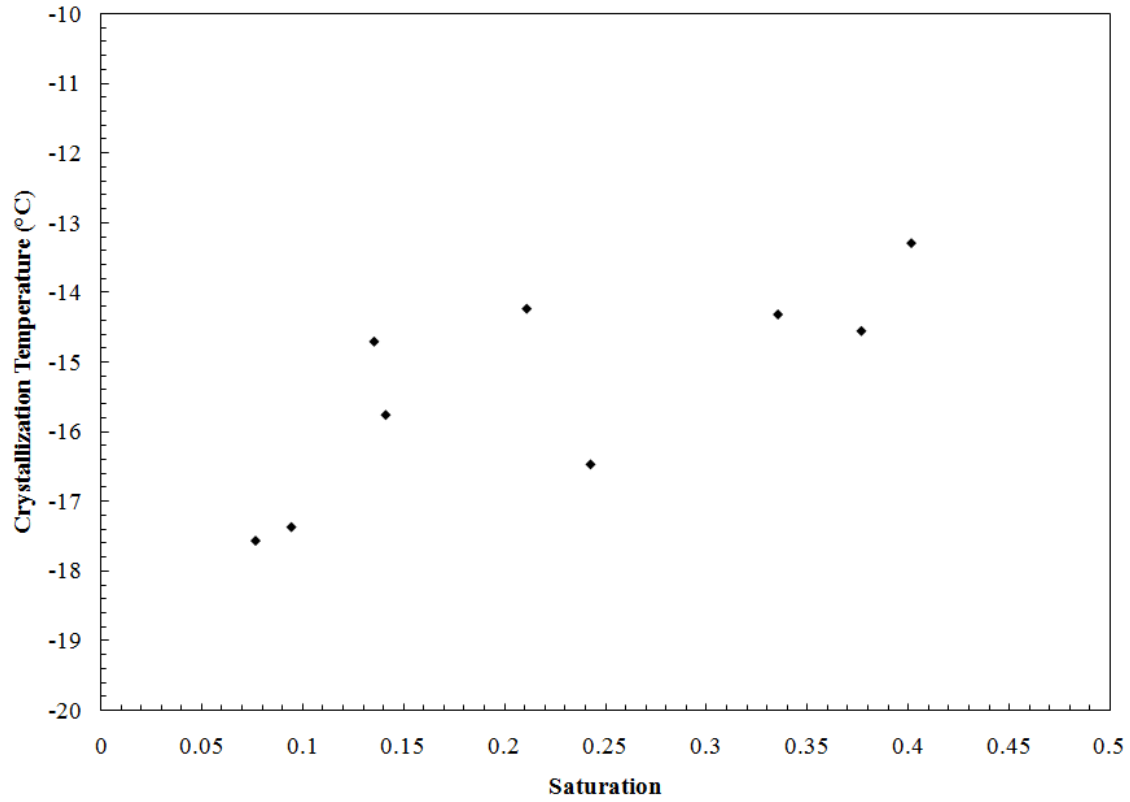
Figure 4. Crystallization temperature versus saturation for an untreated (0 wt % PTFE) Toray GDL from by differential scanning calorimetry.

Theory

To understand the role of GDL wettability (i.e. the PTFE loading) and water saturation, we adopt classical nucleation theory. For crystallization of a sub-cooled liquid in a porous medium, the efforts of Turnbull and Fischer (9) and Bartell (10) were extended by Scherer (11) to give the rate expression

$$ r_f = \frac{4\pi}{9} \left[\frac{2\gamma_{ice/water}\hat{v}_{ice}T_0}{\left|\Delta\hat{H}_f\right|\Delta T} \right]^3 \frac{RT}{\hat{v}_{ice}^2\pi\eta} \exp\left[-\frac{\Delta G^*}{RT} \right] $$

[2]

where r_f is the rate of ice nuclei forming per unit volume of liquid, $\Delta \hat{H}_f$ is the heat of fusion of water, $\gamma_{ice/water}$ is the ice/water surface tension, $\hat{v}_{ice}$ is the molar volume of ice, η is the liquid viscosity, T_0 is the normal freezing point of water (273.15 K), R is the gas constant, and $\varDelta T$ is the sub-cooling defined as T_0-T. For a partially saturated porous medium, the maximum Gibbs free energy barrier, $\varDelta G^*$, is

$$\Delta G^* = \frac{4\pi \gamma_{ice/water}^2 (2 + \cos\theta)(1 - \cos\theta)^2}{3\left[\dfrac{\left|\Delta \hat{H}_f\right|\Delta T}{\hat{v}_{ice}T_0} - \left(1 - \dfrac{\hat{v}_{water}}{\hat{v}_{ice}}\right)p_c\right]^2} \qquad [3]$$

where p_c is the capillary pressure defined as the gas minus liquid pressure and θ is the internal ice/substrate contact angle (measured through the ice phase) given as a function of the PTFE content by Cassie's law as

$$\cos\theta = f_T \cos\theta_T + (1 - f_T)\cos\theta_C \qquad [4]$$

where θ_T is the ice/PTFE contact angle assumed to be 100°, θ_C is the ice/carbon contact angle assumed to be 20°, and f_T is the fraction of PTFE.

For a given contact angle and water saturation, Equations 2 and 3 give a maximum in the rate as a function of sub-cooling temperature (11). By assuming that the temperature corresponding to that maximum rate is characteristic of the freezing temperature in the GDL, Figure 5 shows the predicted crystallization temperature versus the internal ice/substrate contact angle from classical nucleation theory.
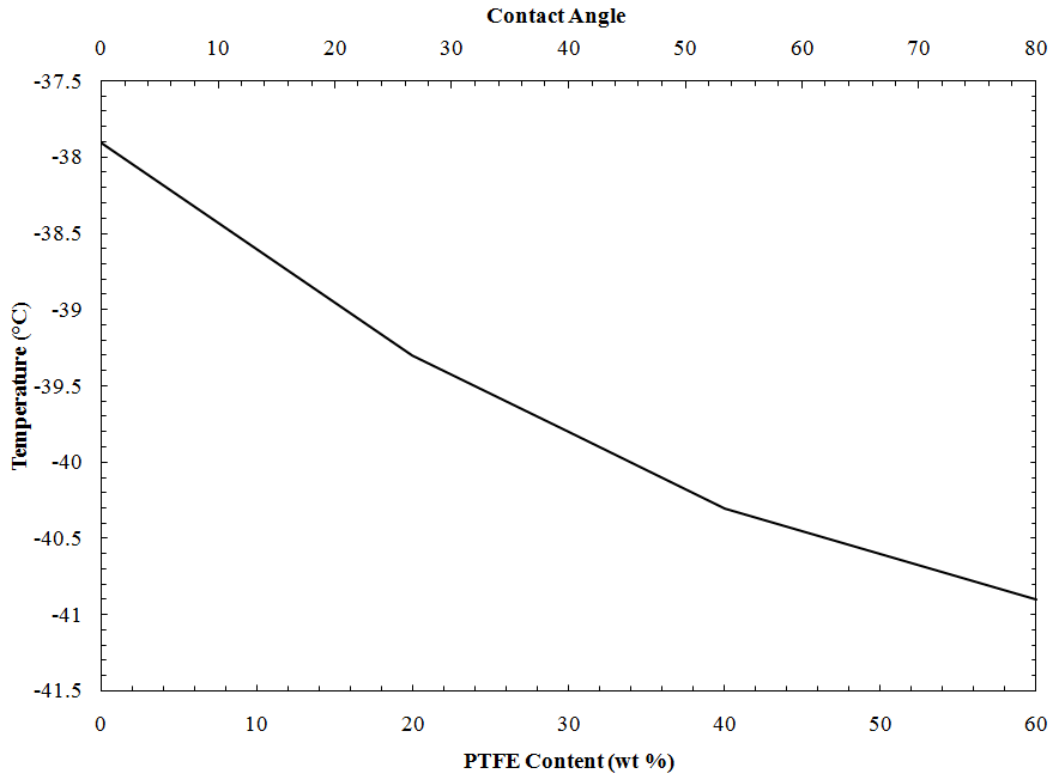

Figure 5.   Crystallization temperature versus internal ice/substrate contact angle as predicted by classical nucleation theory (Equations 2, 3, and 4).

As the PTFE content/contact angle increases, the crystallization temperature decreases. The predicted 3 °C decrease in crystallization temperature over the 0 to 50 wt % Teflon[®]

content is in agreement with the experimental decrease in temperature found by DSC. However, the experimentally measured crystallization temperatures are consistently higher than those predicted by theory. One possible explanation is that rates slower than the maximum rate are sufficient to rapidly form ice within the GDL. This suggests that the actual crystallization temperature is higher than that at the maximum rate of nucleation.

Conclusions

Differential scanning calorimetry was used to elucidate the effect of hydrophobicity and water saturation on the rate of ice formation within a gas-diffusion layer. We found that as the PTFE content of the GDLs increases, the crystallization temperature decreases due to a change in the average internal ice/substrate contact angle, as well as the level of water saturation within the GDL. Classical nucleation theory qualitatively predicts the trends observed by DSC using a Teflon-content dependent contact angle given by Cassie's law.

Acknowledgements

Laboratory for providing the mercury porosimetry data, and Toray and SGL for providing GDL samples.

References

1. J. P. Meyers, "Fundamental Issues in Subzero PEMFC Startup and Operation." UTC Fuel Cells, DOE Freeze Workshop, February 1, 2005.

2. M. Sundaresan and R.M. Moore, *Journal of Power Sources*, **534**, 145 (2005).

3. K. Tajiri, Y. Tabuchi, and C.-Y. Wang, *J. Electrochem. Soc.*, **B147**, 154 (2006).

4. R. J. Balliet, K. E. Thomas-Alyea, and J. Newman, *ECS Trans.*, **16**, 285 (2008).

5. S. He and M. M. Mench, J. *Electrochem. Soc.*, **153**, A1724 (2006).

6. H. Meng, *Journal of Power Sources*, **141**, 178 (2008).

7. J.T. Gostick, M. Fowler, M. Loannidis, and A. Sakars, *J. Phys. Sci.,* **187**, 487 (2009).

8. C. Lim and C.Y. Wang, *Electrochimica Acta*, **4149**, 49 (2004).

9. J. C. Fisher and D. Turnbull, *Journal of Chemical Physics*, **71**, 17 (1949).

10. L.S. Bartell and T.S. Dibble, *J. Phys. Chem.* **1159**, 95 (1991).

11. G.W. Scherer, *Journal of Non-Cryst. Solids*, **1**, 155 (1993).